

1 **Evaluation of Photografted Charged Sites Within Polymer**
2 **Monoliths in Capillary Columns Using Contactless**
3 **Conductivity Detection.**

4
5 **Damian Connolly^a, Vincent O'Shea^b, Paul Clark^b,**
6 **Brendan O'Connor^b and Brett Paull^{a*}**

7
8 **Centre for Bioanalytical Sciences, School of Chemical Sciences^a, School of**
9 **Biotechnology^b, Dublin City University, Glasnevin, Dublin 9, Ireland**

10
11 ***Corresponding author**

12 **Email: Brett.Paull@dcu.ie**

13 **Fax: +353-(0)1-7005503**

14
15
16
17
18
19
20 **Keywords: Polymer monolithic phase; Photografted protein; Contactless**
21 **conductivity detection.**

25 **Abstract.**

26

27 Capacitively coupled contactless conductivity detection (C^4D) is presented as a novel
28 and versatile means of visualising discrete zones of charged functional groups grafted
29 onto polymer based monoliths. Monoliths were formed within 100 μm UV transparent
30 fused silica capillaries and photografting methods were subsequently used to graft a
31 charged functional monomer, 2-acrylamido-2-methyl-1-propanesulfonic acid (AMPS)
32 onto discrete regions of the “generic” monolith using a photomask. Post-modification
33 monolith evaluation involves scanning the C^4D detector along the length of the
34 monolith to obtain a profile of the exact spatial location of grafted charged
35 functionalities with millimetre accuracy. The methodology was extended to the
36 visualisation of several zones of immobilised protein (bovine serum albumin) using
37 photografted azlactone groups to enable covalent attachment of the protein to the
38 monolith at precise locations along its length. In addition, the extent of non-specific
39 binding of protein to the ungrafted regions of the monolith due to hydrophobic
40 interactions could be monitored as an increase in background conductivity of the
41 stationary phase. Finally, the technique was cross-validated using fluorescence
42 microscopy by immobilising green fluorescent protein (GFP) in discrete zones and
43 comparing the profiles obtained using both complementary techniques.

44

45

46 **1. Introduction.**

47

48 A number of recent **publications**^{1 2 3 4} have demonstrated the use of
49 photolithographic methodologies for the modification of pre-formed monolithic
50 stationary phases. Essentially, this procedure involves filling the pores of a monolith
51 with a reactive functional monomer in the presence of a free radical initiator and an
52 inert solvent. By blocking off all but a specific region of the monolith with a photo-
53 mask, irradiation of that particular unmasked region through the UV transparent
54 capillary walls with UV light, will excite the initiator and trigger the covalent grafting
55 of functional groups onto an otherwise inert monolith backbone. This technique
56 thereby results in the simple preparation of monoliths with co-contiguous chemistries,
57 with for example, a generic hydrophobic monolith backbone in one region of the
58 column, and a separate region of the monolith possessing a different grafted
59 functional group such as an anion exchange moiety. Grafted groups can be anion
60 exchange, cation exchange, or protein immobilised via grafted reactive functional
61 monomers such as vinyl azlactone. **[REF 4]**. The benefits of photografting are
62 numerous and have been discussed in a recent comprehensive review by Svec⁵ **[and 3]**

63

64 Modification of polymer monoliths with protein for use as affinity
65 chromatography phases is generating considerable interest. Examples include the
66 immobilisation of protein A, for the separation of immunoglobulins^{6 7 8}, lectins such as
67 concavalin A, for the extraction of glycoproteins⁹, enzymes such as trypsin, for use as
68 micro-bioreactors in LC-MS proteomic applications **[4]** and the immobilisation of
69 immunoglobulins¹⁰. These varied applications of polymeric monolithic stationary
70 phases for affinity chromatography has been the subject of a recent review by **Mallik**

71 **et al**¹¹, in which the numerous immobilisation strategies which have previously been
72 reported are discussed. The most common approaches result in covalent attachment of
73 the protein to monolith and include the epoxy method^{12 13}, the Schiff base method
74 [10,12],[7] the glutaraldehyde method[7]¹⁴, the carbonyldiimidazole method[7,10,12],
75 the disuccinimidyl method, the hydrazide method[10], and the cyanogen bromide
76 method.

77

78 A number of the above immobilisation strategies suffer from a range of
79 disadvantages, including long reaction times, multiple reaction steps, low amounts of
80 immobilised ligand, unwanted side reactions, the use of harsh reagents (which can
81 often cause partial unfolding or complete denaturation of certain proteins) and the use
82 of toxic reagents (cyanogen bromide). Recently, a number of research laboratories
83 have reported the use of vinyl azlactone as an intermediate functional group for the
84 safe and rapid immobilisation of proteins on monolithic surfaces. Vinyl azlactone has
85 previously been covalently attached to monolithic surfaces using the photografting
86 techniques previously discussed, and used as a scavenger for excess amines in
87 reaction mixtures^{15, 16}. Leading on from this, other reports have demonstrated the
88 ability of the azlactone functionality of these monoliths to react readily with
89 nucleophiles such as the amino or thiol groups of proteins thereby enabling their rapid
90 and efficient immobilization via a dipeptidic linker. **[3]**. The advantage of using
91 azlactone chemistry for immobilisation of protein, is that the procedure is rapid
92 (grafting of azlactone takes up to 10 minutes, and the subsequent protein
93 immobilisation takes less than three hours), and the procedure is separated into to
94 steps such that the protein is never in contact with potential denaturants. Considerably
95 higher activity of immobilised ligand has also been reported.

96

97 Obtaining qualitative and quantitative information regarding immobilised
98 protein on surfaces is certainly a challenge. The ability to validate the exact spatial
99 location of immobilised protein and the immobilised quantity thereof on a surface is
100 important and techniques such as surface plasmon resonance^{17 18} ellipsometry,¹⁹
101 optical waveguide lightmode spectroscopy²⁰ and quartz crystal microbalance²¹ have
102 been previously reported. These techniques quantitatively measure the amount of
103 protein immobilised on flat, planar surfaces such as glass, gold and plastic substrates,
104 but these methods cannot easily be utilised for macroporous monolithic materials,
105 because of the huge disparity between the surface area of a monolith compared with a
106 flat surface.

107

108 A relatively new methodology which has not yet been explored as a means of
109 measuring immobilised protein on monoliths is capacitively coupled contactless
110 conductivity detection (referred to hereafter as C⁴D). The principles of C⁴D have been
111 well studied^{22 2324252627}, and the electronic circuitry has been found to be simple and of
112 low cost. The advantage of C⁴D over conventional conductivity detection for
113 chromatography is that the cell design is extremely robust and there is a lack of
114 physical contact with the eluent. This eliminates possible fouling of the electrodes and
115 reduces to zero the extra-column band broadening that would be observed with a
116 conventional conductivity flow cell.

117

118 Building upon results recently reported by this research group,^{28 29}, this paper
119 reports for the first time the use of C⁴D as a novel means of (a) non-invasively
120 inspecting the longitudinal homogeneity of monolithic structure and porosity within

121 capillary formats, (b) visualising the exact location of discrete zones of photografted
122 charged functionalities or immobilised protein on polymer monoliths and (c) the semi-
123 quantitative evaluation of non-specific binding of protein to hydrophobic monoliths
124 before, during and after column washing steps.

125

126 **2. Experimental.**

127

128 **2.1 Instrumentation.**

129

130 The pump used for washing and equilibration of monoliths, for immobilisation
131 of proteins (BSA and GFP-His) and during the taking of conductivity readings was a
132 Dionex Ultimate 3000 LPG 3000 pump (Dionex, Sunnyvale, California). The
133 operational flow rate was 1 $\mu\text{L}/\text{min}$. The pump used to prepare monolithic columns
134 and to fill the pores of pre-formed monoliths with reactive monomers for photo-
135 grafting was a Knauer pump Model K120 operated at 10 $\mu\text{L}/\text{min}$. The detector used
136 was a TraceDec capacitively coupled contactless conductivity detector (Innovative
137 Sensor Technologies GmbH, Innsbruck, Austria). The exact position of the detection
138 cell along the length of the monolithic column was varied by hand, using a ruler as a
139 position indicator. The monolithic column itself was passed through the radial
140 capillary detector cell, which was programmed with the following settings: frequency,
141 3X HIGH; voltage, -12 dB; gain, 50% and offset, 0. A GFL water bath was used for
142 monolith production, and the operational temperature was 60 $^{\circ}\text{C}$. A Labnet
143 Spectrafuge centrifuge was used to eliminate particulate matter during the preparation
144 of monomer solutions and protein solutions. The UV lamp used was a Bondwand
145 (Electro-Lite Corporation, Conneticut, USA) for production of monoliths with
146 differing regions of porosity, and for photo-grafting of 2-acrylamido-2-methyl-1-

147 propanesulfonic acid onto pre-formed monoliths. The operational wavelength of this
148 lamp was 350 nm with an irradiation intensity of 10 mW/cm². The UV lamp used for
149 photografting of 4,4-dimethyl-2-vinylazlactone onto methacrylate monoliths was a
150 battery operated handheld UVP lamp, model UVG4 with an operational wavelength
151 of 254 nm with an irradiation intensity of 170 μW/cm² at 3". The photomask used for
152 production of monoliths with differing zones of porosity was simply some black
153 electrical tape stuck down over the capillary such that the photomask was only one
154 layer thick (of tape). For all other photomasking events, the capillary monolith was
155 passed through short pieces of 1/16" PEEK tubing (i.d. 380 μm). SEM images were
156 taken with a Hitachi S-3000N scanning electron microscope. Fluorescence
157 microscopy images were taken with the aid of a Vilber Lourmat UV Transluminator
158 at wavelength of 254 nm and with a Panasonic NV-GS500 40 Megapixel digital video
159 camera with 12X optical zoom.

160

161 **2.2 Reagents.**

162

163 Butyl methacrylate (99%, BuMA), ethylene dimethacrylate (98%, EDMA),
164 benzophenone (99+%, BP), 3-(trimethoxysilyl)- propyl methacrylate (98%), AIBN,
165 1,4-butanediol, *tert*-butyl alcohol (99.5%), 2-acrylamido-2-methyl-1-propanesulfonic
166 acid, sodium sulphate, sodium carbonate, bovine serum albumin (BSA) and sodium
167 hydroxide pellets were purchased from Sigma-Aldrich (Tallaght, Dublin, Ireland).
168 Hydrochloric acid was purchased from Fluka. Vinyl azlactone (4,4-dimethyl-2-
169 vinylazlactone) was purchased from TCI Europe. Methanol, acetone and 1-propanol
170 were purchased from Labscan (Stillorgan, Dublin, Ireland). All other reagents were of
171 the highest available purity and used as received without additional purification or

172 distillation before use. UV transparent teflon coated fused silica capillary (100 μm i.d.)
173 was obtained from Polymicro Technologies (Phoenix, AZ). Deionised water was
174 produced with a Millipore Direct-Q™ 5 (Millipore, Bedford, MA, USA) water
175 purification system, and eluents were vacuum filtered through a 0.2 μm filter (Supelco,
176 Supelco Park, Bellefonte, PA, USA) and degassed by sonication. The eluent used for
177 immobilisation of BSA and GFP-His was 0.5 *M* sodium sulphate, 0.1 *M* sodium
178 carbonate at a flow rate of 1 $\mu\text{L}/\text{min}$. Histidine tagged green fluorescent protein (GFP-
179 His) was expressed in *E. coli* and purified using nickel affinity chromatography.

180

181 **2.3 Vinylisation of fused silica capillaries for monolith production.**

182

183 A suitable length of fused teflon-coated silica capillary (100 μm i.d.), was
184 rinsed with acetone using a pump at 10 $\mu\text{L}/\text{min}$, and dried in a stream of nitrogen for
185 10 minutes at room temperature. The inner walls of the capillary were then activated
186 with 0.2 mol/L sodium hydroxide for 30 minutes by pumping at 10 $\mu\text{L}/\text{min}$. The
187 capillary was then washed in the following order at 10 $\mu\text{L}/\text{min}$: water for 5 minutes,
188 0.2 mol/L HCl for 30 minutes, water for 5 minutes, and finally with acetone for 5
189 minutes. After drying the capillary again with nitrogen gas, a 50 wt % solution of 3-
190 (trimethoxysilyl)propyl methacrylate in acetone was prepared. A 435 μL length of
191 PEEK tubing was then filled with the solution using a disposable syringe, one end of
192 the filled loop was attached to the empty capillary, and the other end to the outlet of a
193 piston driven pump delivering methanol at 10 $\mu\text{L}/\text{min}$. The reagent was pumped
194 through the capillary at 10 $\mu\text{L}/\text{min}$ until all air was expelled from the capillary and the
195 entire capillary length was full of reagent. The capillary was then end-capped with
196 pieces of rubber septa, and immersed in a water bath at 60 °C for 20 hours. Finally,

197 the column end-plugs were removed, the column was flushed with acetone to remove
198 excess 3-(trimethoxysilyl)propyl methacrylate, and the column was dried with a
199 stream of nitrogen and stored indefinitely.

200

201 **2.4 Preparation of methacrylate monolithic capillary columns.**

202

203 A polymerization mixture was prepared comprising 24 % BuMA, 16 %
204 EDMA, 34 % 1-propanol, 26 % 1,4-butanediol, and 0.4 % AIBN as free radical
205 initiator (all w/w). The solution was sonicated for 20 minutes to dissolve the AIBN,
206 and then centrifuged for 10 minutes at 13,000 r.p.m to eliminate particulate matter.
207 The supernatant was degassed by allowing nitrogen gas to bubble through the solution
208 for 10 minutes. The de-aerated monomer solution was introduced into the capillary
209 using a PEEK loop as described above, and each end of the capillary again sealed
210 with a piece of rubber. Monoliths were prepared using either thermal or
211 photochemical initiation. The former was carried out by immersing the capillaries in a
212 water bath kept at 60 °C for 20 hours, while photoinitiated polymerizations in the UV
213 transparent Teflon-coated capillaries required irradiation using a Bondwand UV lamp
214 at 350 nm and a distance of 5 centimetres for one hour. After removing the seals, the
215 columns were flushed with methanol at a flow rate of 1 µL/min for 60 min to remove
216 porogen and unreacted monomer using the Dionex LC pumping system.

217

218 **2.5 Photografting of porous methacrylate monoliths with 2-acrylamido-2-** 219 **methyl-1-propanesulfonic acid (AMPS).**

220

221 A mixture comprising 15 wt% AMPS and 0.22 wt% benzophenone in a
222 porogen comprising 75/25 t-butanol/water was prepared and vortexed vigorously to
223 dissolve the solid material. After centrifuging at 13,000 r.p.m for 10 minutes, the
224 supernatant was degassed with nitrogen for 10 minutes. The de-aerated solution was
225 pumped through the methacrylate monolith to completely fill the pores using the
226 PEEK loop and pump as previously described. The column was then end-capped with
227 rubber and photo-grafting was achieved by irradiating the column through a number
228 of precisely positioned PEEK photo-masks (of approximately 10 mm in length) at a
229 wavelength of 350 nm at a distance of 5 cm for one hour. The capillary was then
230 washed with methanol at a flow velocity of 1 μ L/min for 12 hours, followed by water
231 for 3 hours.

232

233 **2.6 Photografting of porous polymer monoliths with 4,4-dimethyl-2-** 234 **vinylazlactone.**

235

236 The same procedure was used as for photografting of 2-acrylamido-2-methyl-
237 1-propanesulfonic acid, except that the monomer solution comprised 15 wt% 4,4-
238 dimethyl-2-vinylazlactone and 0.22 wt% benzophenone in a porogen comprising
239 75/25 t-butanol/water. The UV lamp used was a UVP battery operated lamp at 254
240 nm, with the face of the lamp in constant contact with the region of capillary not
241 covered by the photomask. The time of irradiation was 30 minutes. The capillary was
242 then washed with methanol at a flow velocity of 1 μ L/min for 2 hours, followed by
243 water for 3 hours.

244

245 **2.7 Immobilisation of proteins on azlactone functionalised monoliths.**

246

247 For immobilisation of each particular protein (bovine serum albumin or GFP-
248 His), each protein was prepared as a 1 mg/ml solution in 0.5 M sodium sulphate and
249 0.1 M sodium carbonate. A washed 435 μ L loop was filled with the protein solution
250 (BSA or GFP-His) using a manual syringe, and one end of the loop connected to the
251 azlactone functionalised monolith, with the opposite end connected to the Dionex LC
252 pumping system which was primed with 0.5 M sodium sulphate / 0.1 M sodium
253 carbonate. The protein solution was pumped through the monolith at 1 μ L/min for
254 three hours at room temperature to allow covalent attachment of the protein to the
255 azlactone functionalities via native lysine or cysteine groups on the protein surface.
256 After immobilisation, the column was washed with water for up to 3 hours at 1 μ L/min.

257

258 **2.8 Verification of the presence of charged groups on functionalised** 259 **monoliths using C⁴D.**

260

261 While pumping water through the functionalised monolith at 1 μ L/min, the
262 detection cell was physically scanned across the length of the column at millimetre
263 increments to allow the detection of localised regions of charge within the monolithic
264 stationary phase. The conductivity value (reported as mV) at each millimetre location
265 along the column was recorded. C⁴D was also used in the same manner to locate the
266 presence of voids/regions of diffuse porosity within a length of otherwise
267 homogeneous monolithic stationary phase.

268

269 **2.9 Cross-validation of the C⁴D methodology using fluorescence microscopy.**

270

271 Monolithic columns containing a number of zones of immobilised GFP-His,
272 were flushed with methanol to remove non-specifically bound protein, and placed on
273 the plate of a Vilber Lourmat UV transluminator, which irradiated the monolithic
274 columns from below with light of 254 nm. Photographic images of monoliths
275 illuminated in this manner were taken with a Panasonic digital video camera as
276 described.

277

278 **3. Results and discussion.**

279

280 **3.1 Evaluation of monolith quality using C⁴D.**

281

282 The monolithic stationary phase was produced using the procedure of Geiser
283 et al³⁰. Butyl methacrylate was specifically chosen as a monomer since it exhibits
284 appreciable hydrophobic character, and therefore should result in non-specific binding
285 of protein in ungrafted regions of the monolith. Butyl methacrylate would also not
286 significantly contribute to background conductivity measurements since it does not
287 contain ionisable groups. Prior to monolith formation, capillaries were wall-modified
288 as described in Section 2.3. Monolith formation was carried out as detailed in Section
289 2.4. The hydrodynamic properties of the monolith formed were adequate for the
290 purposes of this work, with for example a 12 cm x 100 µm monolith producing a
291 backpressure of 4 bar while pumping water at 1 µL/min. The above recipes for
292 generic monolith production were found to be both robust and reproducible. The
293 hydrodynamic properties were not extensively studied since the primary aim of this
294 work was to use C⁴D to detect zones of different charged functionalities or zones of
295 differing porosity *within the same single monolith*.

296

297 Determination of monolith pore size and the location of monolith breakages or
298 voids is an important quality control test for laboratories producing monolithic
299 columns. The pore size dictates the hydrodynamic properties of a monolith, with large
300 pore sizes resulting in lower backpressures at a given flow rate for a given solvent, but
301 with concomitantly lower surface area. Typically, the pore structure of a monolith is
302 determined using two complementary methodologies. The first involves the use of
303 scanning electron microscopy which is a destructive technique in that the column
304 needs to be sliced into cross-sections before microscopic analysis, with the images
305 typically used to confirm that the monolith is well bound to the wall. In addition,
306 SEM images are generally used to directly compare two or more monoliths produced
307 under different conditions such as porogen type, porogen concentration, reaction time,
308 reaction temperature etc. Secondly, for the determination of actual average pore size
309 within a monolith or the pore size distribution, such techniques as mercury-intrusion
310 porosimetry are often applied. [4]

311

312 Neither of the above common techniques allows a non-invasive evaluation of
313 the longitudinal homogeneity and structural uniformity of the monolith within the
314 capillary column. However, C^4D can be recorded along the entire length of a column
315 non-invasively, with the recorded response directly proportional to sum of conducting
316 elements within the 'virtual electrode area' [30-35] [45]. The presence of non-
317 conducting monolithic phase filled with a background solution, housed within a fused
318 silica capillary of uniform character, will provide a conductive response proportional
319 to the fluid volume. Hence, where irregularities within the monolith structure exist,
320 these will be apparent in the C^4D capillary profile. In this study a monolithic column

321 was produced containing four separate zones in which the monolith was drastically
322 diffuse relative the remainder of the monolith. This was achieved using a photo-
323 initiated polymerisation technique whereby the fused silica capillary containing the
324 monomer mix, was masked in four discrete regions with pieces of black electrical tape,
325 with each masked region measuring approximately 10 to 13 millimetres. After
326 irradiating the UV transparent capillary for one hour at a distance of 5 centimetres, a
327 monolith was obtained containing four highly porous zones (it was expected that no
328 monolith at all would form under the masked zones, however partial formation of
329 monolith under each masked region was observed).

330

331 Figure 1 illustrates the C^4D response profile obtained by scanning the detector
332 along the length of the capillary column at one millimetre intervals while pumping
333 deionised water through at 1 μ L/min. The zones where there was “less” monolith are
334 clearly evident and result in higher C^4D responses. There are also present small zones
335 of increased monolithic density at the interface between the photo-masked zones and
336 unmasked regions. Although here these zones represent a minor irregularity in the
337 monolith structure, the C^4D evaluation clearly identifies their presence. Two cross-
338 sectional slices of the monolith were made at approximately 25 mm (sample A) along
339 the monolith and 36 mm (sample B) along the monolith, corresponding to regions of
340 low and high C^4D response respectively, and subjected to SEM evaluation to validate
341 the above C^4D profile. Figure 2 clearly illustrates that sample B contains large voids,
342 consistent with an incomplete polymerisation, whereas sample A exhibits the normal
343 uniformly structured monolith.

344

345 **3.2 Determination of the spatial location of precisely grafted charged**
346 **functionalities (AMPS) using C⁴D.**

347

348 Until now, the visualisation of grafted zones of different functionalities on a
349 single monolith has been challenging and time consuming. If the grafted functional
350 groups are fluorescent, or can be reacted with a fluorescent tag in a second step after
351 photo-grafting is complete, then fluorescence microscopy can be utilised to visualise
352 the grafted zones. **Rohr et al [1]** used this approach recently to visualise grafted zones
353 of vinyl azlactone by tagging the azlactone functionalities with Rhodamine 6G via its
354 secondary amino groups. This methodology also allowed **Rohr et al** to evaluate the
355 sharpness of the boundaries between the grafted and ungrafted zones, which ideally
356 should be perpendicular to the capillary axis. In this manner the irradiation time and
357 the physical geometry of the photomasks employed could be accurately optimised.

358

359 **Gillespie et al [44]** have previously reported the use of C⁴D to detect the
360 presence of hydrophobically adsorbed ionic surfactants on capillary C₁₈ silica
361 monoliths. The same approach was used in this work, but in this case ionisable
362 functional monomers were photo-grafted onto a butyl methacrylate monolith using
363 techniques previously discussed. AMPS (2-acrylamido-2-methyl-1-propanesulfonic
364 acid) was selected as a suitable candidate for grafting since it contains a strong acid
365 sulfonate group which is ionised across the pH range, and because the grafting of this
366 monomer onto polymer monoliths has been well studied. **[1,2]** Figure 3 shows the
367 C⁴D profile of a butyl methacrylate monolith containing two zones of photografted
368 AMPS. The generic “backbone” monolith yields a low conductivity response as
369 expected. Since it is typically desirable to have a sharp graft boundary, it is advantage

370 of this proposed method that the detector can be scanned across the column length
371 with millimetre precision. This results in a very sharp and rapid increase in the
372 conductivity response as the pair of C^4D electrodes pass across the region of monolith
373 where the grafted groups begin, and an equally rapid return to baseline once the
374 moving detector cell has left the tail edge of the grafted zone behind. The uniform
375 baseline conductance shown in Figure 3 surrounding the zones of AMP, illustrates the
376 quality of the pre-formed monolith, whereas the contribution to the conductance from
377 the presence of the charged AMP groups is equally clear. The two separate zones
378 were grafted also to show how C^4D can be used to readily monitor the reproducibility
379 of the photografting process, which in this case is highly reproducible. Although not
380 shown here, it is readily possible to correlate the conductance signal recorded and the
381 density of AMP groups upon the monolith and so also utilise this simple technique to
382 determine 'zone capacity'.

383

384 **3.3 Determination of the precise spatial location of immobilised protein and** 385 **non-specifically bound protein using C^4D .**

386

387 One of the few non-invasive methodologies for both detection and
388 quantification of adsorbed protein on monolithic surfaces has been recently reported
389 by Stachowiak et al³¹. They described a fluorescence assay that was performed “on-
390 monolith” for semi-quantitative determination of fluorescein-labeled bovine serum
391 albumin (BSA), which was allowed to hydrophobically adsorb onto a range of
392 monoliths, the surfaces of which were each grafted with progressively more
393 hydrophilic functional monomers. This allowed them to evaluate the most suitable
394 hydrophilic graft monomers to use for the reduction of unwanted non-specific binding

395 of proteins to monolithic surfaces. Stachowiak et al. pointed out that a limitation of
396 the methodology was that the fluorescence intensity was not directly proportional to
397 the absolute amount of adsorbed protein and so the method was not strictly
398 quantitative, but could nevertheless be used for making simple comparisons between
399 monolithic surfaces using the same model protein.

400

401 Here, having successfully visualised the exact spatial location of grafted
402 charged functional groups on an otherwise electrically neutral monolith using C^4D , it
403 follows that the same methodology should permit the detection of immobilised protein
404 on a surface. All immobilised proteins will carry a net charge at given pH due to the
405 presence on their surface of amino acids with ionisable R-groups such as lysine,
406 arginine, glutamic acid and aspartic acid. It follows therefore that the passage of the
407 C^4D detector cell across a monolithic surface on which protein is immobilised at
408 specific locations should result in an increase in signal at each protein immobilisation
409 zone due to the native net charge of that protein. Therefore, a monolith containing two
410 9 mm long photografted zones of vinyl azlactone was flushed with a solution of 1
411 mg/ml bovine serum albumin (BSA) in 0.5 M sodium sulphate, 0.1 M sodium
412 carbonate at a flow rate of 1 μ L/min for 3 hours. A high salt carrier solution was used
413 to facilitate covalent attachment of BSA to the azlactone modified support, based on
414 the findings of **Drtna et al.**³² After washing the column extensively with water, the
415 C^4D detector was scanned across the column as described, and a profile obtained as
416 shown in Figure 4 (Profile a). Again, the presence of two narrow well-defined zones
417 of immobilised BSA can be clearly seen, with the width of each zone matching
418 perfectly with the original width grafted azlactone zones (9 millimetres). A significant
419 advantage of this technique over that developed by Stachowiak et al. is that it is not

420 necessary to fluorescently tag the protein prior to immobilisation, which may
421 negatively impact secondary interactions in affinity applications.

422

423 In the evaluation of bound protein on affinity monoliths, produced in the
424 above manor, it is important to be able to readily distinguish non-specifically
425 bound/adsorbed protein. C⁴D offers a simple and semi-quantitative method to evaluate
426 the spatial location of non-specifically bound protein on such a monolith. As
427 previously discussed, butyl methacrylate was used as a monomer to produce the
428 backbone monolith, since it has appreciable hydrophobic character that would
429 promote non-specific hydrophobic binding of protein across the entire length of the
430 column. Bovine serum albumin is well known as an adhesive protein that binds to a
431 wide variety of surfaces. Figure 4 illustrates that non-specific binding of protein has
432 taken place. The profile with the lowest conductivity (Profile d) was obtained after the
433 azlactone groups had been photo-grafted to the butyl methacrylate support followed
434 by copious washing with water, but *before* BSA had been immobilised. After
435 immobilisation of BSA, Profile (a) was obtained. Profile (a) demonstrates that as well
436 as the presence of two distinct zones of covalently immobilised BSA via azlactone
437 groups, the overall conductivity of the stationary phase across the entire length of the
438 column has shifted higher (300 to 400 mV). This is clearly due to non-specific
439 binding of BSA to the non-grafted regions of the butyl methacrylate monolith through
440 hydrophobic interactions. Profile (b) shows that the amount of non-specifically bound
441 BSA had been reduced after further copious washing with water. Profile (c) was
442 obtained after washing the column with methanol and shows that the conductivity of
443 the stationary phase had been reduced down to the original value prior to
444 immobilisation of BSA (Profile d). This clearly indicates that the high conductivity

445 value across the length of the column was due to hydrophobic interactions, which
446 were disrupted by flushing the column with an organic solvent. It is also indicative of
447 the fact that the immobilised zones of BSA were covalently bound to the grafted
448 azlactone functionalities, with this covalent bond undisturbed by the presence of
449 organic modifiers. It is proposed that the absolute conductivity of both immobilised
450 zones of BSA was reduced due to excessive washing with water and finally methanol,
451 because some of the BSA present in those zones was non-specifically bound, causing
452 a net increase in conductivity in that particular zone when combined with the
453 covalently immobilised BSA via the azlactone moiety.

454

455 **3.3 Cross-validation of the C⁴D methodology using fluorescence microscopy.**

456

457 The use of C⁴D detection for the profiling of monolithic columns containing
458 discrete zones of immobilised protein was cross-validated with an orthogonal
459 methodology. Green fluorescent protein (GFP) was immobilised on a monolith which
460 had three separate zones of grafted azlactone groups, and then extensively washed
461 with methanol to remove any non-specifically bound protein due to hydrophobic
462 interactions. While pumping water at 1 μ L/min, the C⁴D response profile was
463 collected and is shown as Figure 5(b). After the C⁴D profile was acquired, the
464 monolithic column (with attached scale bar) was placed on the bed of a UV
465 transilluminator set to a wavelength of 254 nm and a digital image was captured,
466 which is shown aligned with the C⁴D response as Figure 5(a). The position of three
467 sharp zones of immobilised GFP are clearly visible, represented as bright fields within
468 the monolith. The sharp boundary between the regions of the monolith containing
469 grafted zones of azlactone and therefore immobilised GFP, and the ungrafted

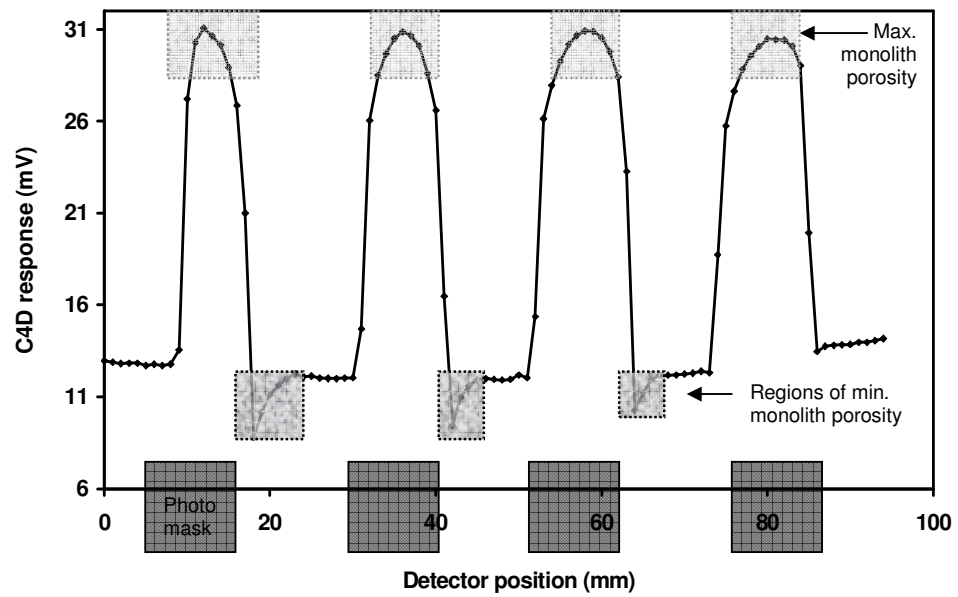
470 monolith regions is clear from both Figure 5(a) and 5(b). However, the C⁴D profile
471 provides additional information about the protein zones, including the longitudinal
472 homogeneity of the protein band itself, which here clearly shows the highest protein
473 concentration towards the centre of the zone, and secondly the means for quantitative
474 evaluation of each bound protein zone, in terms of peak area and height measurements.
475 Here, the C⁴D profiles shown allow a simple and rapid determination of an
476 approximate 5-10% lower amount of bound protein in zone three in comparison with
477 zones 1 and 2.

478

479 **4 Concluding remarks.**

480

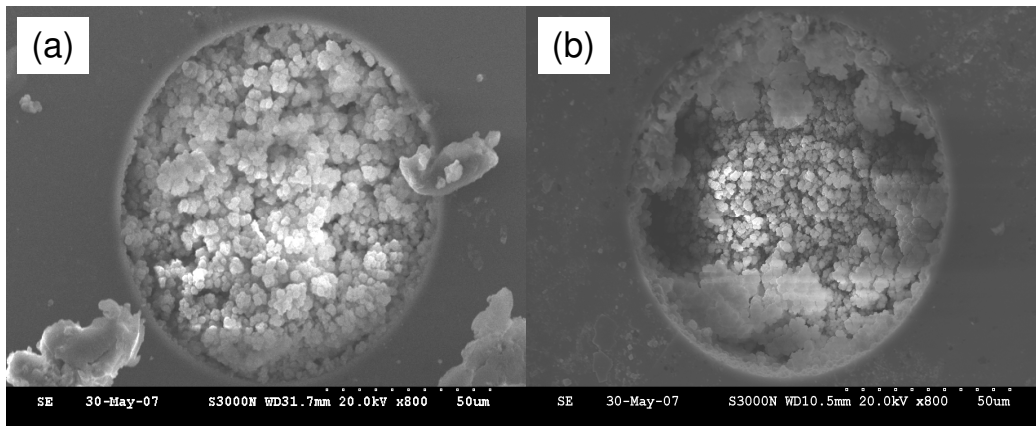
481 A novel use of a simple, inexpensive commercially available technology (C⁴D)
482 has been presented as a means of rapidly profiling the presence of charged groups
483 covalently bound to monolithic stationary phases housed within capillary columns.
484 The use of this technique has been demonstrated to be particularly useful as a means
485 of detecting the precise location and homogeneity of photografted immobilised
486 protein, together with the precise location and extent of non-specific binding of
487 unwanted protein. Application of C⁴D in this way should therefore facilitate future
488 evaluation of affinity monolith fabrication techniques by allowing a potentially
489 quantitative scanning profile of a monolith to be established in a matter of minutes.
490 The universal nature of this technique is particularly interesting, since the
491 visualisation of grafted zones of protein is not restricted merely to proteins that
492 fluoresce.



493

494

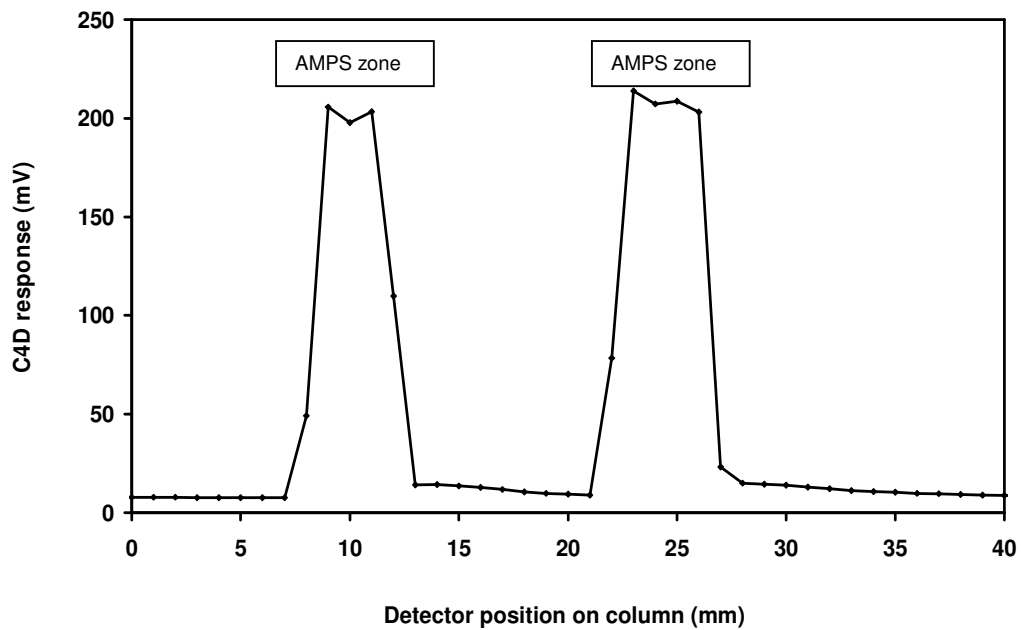
495 **Figure 1.** Porosity profile of a monolith containing four zones of incomplete polymerisation.
 496 Profile acquired while pumping water at 1 $\mu\text{l}/\text{min}$.
 497



498

499

500 **Figure 2.** Scanning electron microscopy images of monolith cross-sections taken (a) 25
501 mm and (b) 36 mm along the length of the capillary column.
502



503

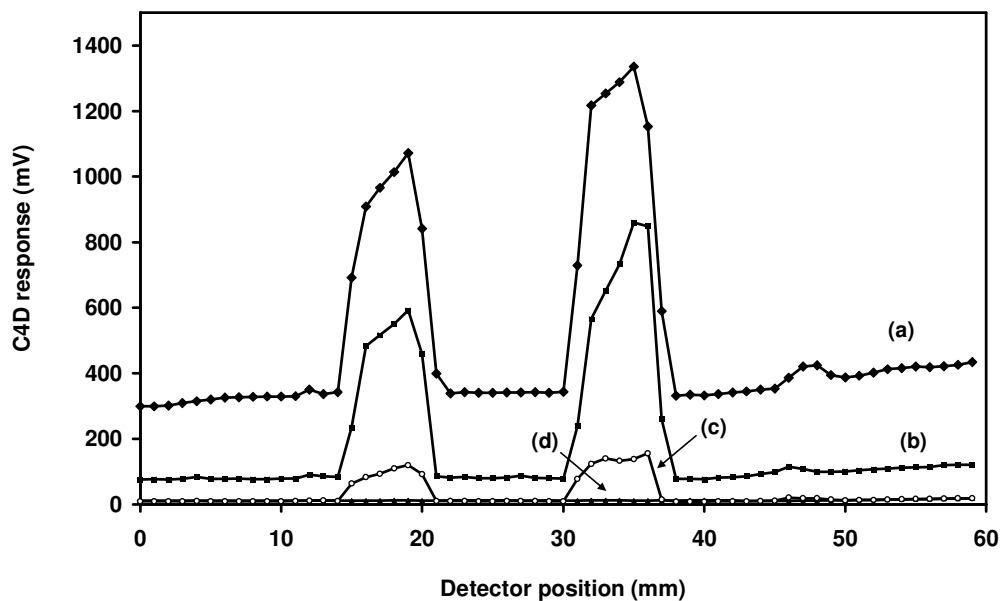
504

505 **Figure 3.** Conductivity profile of a monolith containing two sharp zones of grafted AMPS.

506

Profile acquired while pumping water at 1 μ l/min.

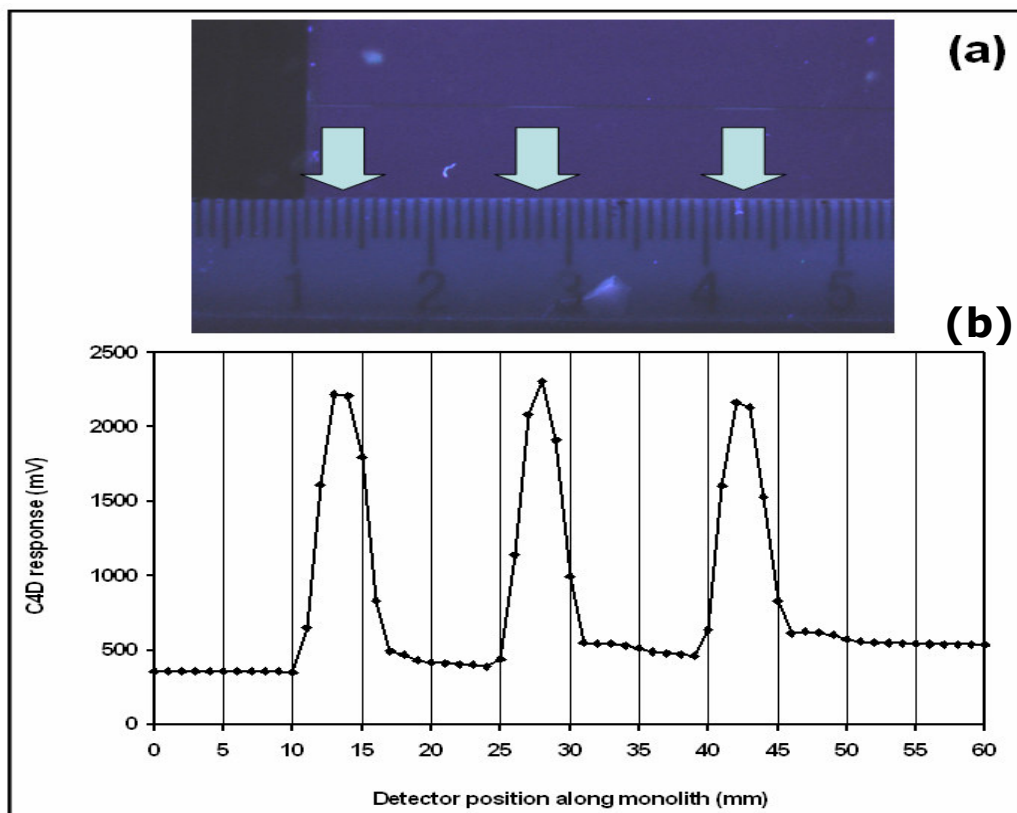
507



508

509

510 **Figure 4.** Conductivity profile of a monolith containing two zones of immobilised bovine serum
 511 albumin (BSA) via a dipeptide linkage via photgrafted vinyl azlactone. Profile (a)
 512 was obtained after washing the BSA immobilised monolith with water for one hour.
 513 Profile (b) was obtained after washing the monolith for a further 24 hours with water.
 514 Profile (c) was obtained after then washing the monolith for one hour with 100 %
 515 methanol. Profile (d) was obtained before immobilisation of BSA.
 516



517
518
519
520
521
522
523
524
525
526
527
528
529

Figure 5. Comparison of fluorescence microscopy image with C^4D conductivity profile for a monolith with three zones of immobilised GFP. Figure 5 illustrates (a) the fluorescent zones of GFP, overlaid and aligned with (b) the zones of increased C^4D response. The dark region in 5(a) left is a section of the C^4D cell, the centre of which is positioned at the zero millimetre location on the capillary.

References

530 **To be updated**

¹Rohr T, Hilder E , Donovan J , Svec F, Fréchet J *Macromolecules* 2003, 36, 1677-1684

²Pucci V, Raggi M, Svec F, Fréchet J, *J. Sep. Sci.* 2004, 27, 779–788

³Svec F, *LC•GC Europe* 2 18(1) 17–20 (2004).

⁴Peterson D, Rohr T, Svec F, Fréchet J *Anal. Chem.* 2003, 75, 5328-5335

⁵Svec F, *J. Sep. Sci.* 2004, 27, 747–766

-
- ⁶ Berruex, L. G., Freitag, R., Tennikova, T. B., *J. Pharm. Biomed. Anal.* 2000, 24, 95–104.
- ⁷ Luo, Q., Zou, H., Zhang, Q., Xiao, X., Ni, J., *Biotechnol. Bioeng.* 2002, 80, 481–489.
- ⁸ Pan, Z., Zou, H., Mo, W., Huang, X., Wu, R., *Anal. Chim. Acta* 2002, 466, 141–150,
- ⁹ D. Josić *et al.* / *J. Chromatogr. A* 803 (1998) 61–71
- ¹⁰ Jiang, T., Mallik, R., Hage, D. S., *Anal. Chem.* 2005, 77, 2362–2372.
- ¹¹ Mallik R, Hage S, *J. Sep. Sci.* 2006, 29, 1686 – 1704
- ¹² Mallik, R., Jiang, T., Hage, D. S., *Anal. Chem.* 2004, 76, 7013–7022.
- ¹³ Kim, H. S., Hage, D. S., in: Hage, D. S. (Ed.), *Handbook of Affinity Chromatography*, CRC Press, Boca Raton 2005, Chapter 3,
- ¹⁴ Petro, M., Svec, F., Frechet, J. M. J., *Biotechnol. Bioeng.* 1996, 49, 355–363,
- ¹⁵ Tripp J, Svec F, and Frechet J J. *Comb. Chem.* 2001, 3, 216-223
- ¹⁶ Tripp J, Stein J, Svec F, Frechet J *Org. Lett.*, Vol. 2, No. 2, 2000
- ¹⁷ Ostuni, E.; Yan, L.; Whitesides, G. M. *Colloids Surf., B* 1999, 15, 3-30.
- ¹⁸ Green, R. J.; Frazier, R. A.; Shakesheff, K. M.; Davies, M. C.; Roberts, C. J.; Tandler, S. J. B. *Biomaterials* 2000, 21, 1823-1835.
- ¹⁹ Elwing, H. *Biomaterials* 1998, 19, 397-406,
- ²⁰ Vořroš, J.; Ramsden, J. J.; Csúcs, G.; Szendro, I.; De Paul, S. M.; Textor, M.; Spencer, N. D. *Biomaterials* 2002, 23, 3699-3710.
- ²¹ Čyavić, B. A.; Hayward, G. L.; Thompson, M. *Analyst* 1999, 124, 1405-1420,
- ²² A.J. Zemann, E. Schnell, D. Volgger and G.K. Bonn, *Anal. Chem.* 70 (1998), p. 563
- ²³ J.A. Fracassi da Silva and C.L. do Lago, *Anal. Chem.* 70 (1998), p. 4339.
- ²⁴ P. Kubáň and P.C. Hauser, *Electrophoresis* 25 (2004), p. 3387.
- ²⁵ P. Kubáň and P.C. Hauser, *Electrophoresis* 25 (2004), p. 3398
- ²⁶ J.G.A. Brito-Neto, J.A.F. da Silva, L. Blanes and C.L. do Lago, *Electroanalysis* 17 (2005), p. 1198.

-
- ²⁷ **J.G.A. Brito-Neto, J.A.F. da Silva, L. Blanes and C.L. do Lago, *Electroanalysis* 17 (2005), p. 1207.**
- ²⁸ **Gillespie E, Macka M, Connolly D Brett Paull B Analyst, 2006, 131, 886–888**
- ²⁹ **O´ Riordain C, Gillespie E, Connolly D, Nesterenko P, Paull B Journal of Chromatography A, 1142 (2007) 185–193**
- ³⁰ **Geiser L, Eeltink S, Svec F, Fr´echet J, Journal of Chromatography A, 1140 (2007) 140–146**
- ³¹ **Stachowiak T, Svec F and Fr´echet J Chem. Mater. 2006, 18, 5950-5957.**
- ³² **Drtna G, Haddad L, Rasmussen J, Gaddam B, Williams M, Moeller S, Fitzsimons R, Fansler D, Buhl T, Yang Y, Weller V, Lee J, Beauchamp T, Heilmann S, *Reactive & Functional Polymers* 64 (2005) 13–24**